

NASA – Final Report

Mitigating Climate Change With Earth Orbital Sunshades

Victoria Coverstone¹
University of Illinois, Urbana, IL, 61801

Les Johnson²
NASA Marshall Space Flight Center, Huntsville, AL, 35816

An array of rotating sunshades based on emerging solar sail technology will be deployed in a novel Earth orbit to provide near-continuous partial shading of the Earth, reducing the heat input to the atmosphere by blocking a small percentage of the incoming sunlight, and mitigating local weather effects of anticipated climate change over the next century. The technology will provide local cooling relief during extreme heat events (and heating relief during extreme cold events) thereby saving human lives, agriculture, livestock, water and energy needs. A synthesis of the solar sail design, the sails' operational modes, and the selected orbit combine to provide local weather modification.

Nomenclature

A_s	= Sun's apparent area
A_{sh}	= area of individual shade, km ²
B	= percentage of blocked solar energy globally
CO_2	= carbon dioxide
GE	= geo-engineering
K	= non-dimensional distance from earth = x/R_e
L_1	= Sun-Earth libration point 1.5x10 ⁶ km away from Earth
R_e	= Earth's average radius = 6378 km
SRM	= Solar Radiation Management
b	= percentage of blocked solar energy locally
$ppmv$	= parts per million by volume
x	= distance between sub-solar point and shade centroid

I. Introduction

Global climate change is a hotly debated topic amongst the American public but many leading scientists believe that the data substantiates the claims that weather patterns are changing. Several National Academy of Science studies correlate global temperature change with the build-up of greenhouse gases, carbon dioxide (CO₂) in particular, in the atmosphere.¹⁻³ The Earth's principal greenhouse gases are water vapor, CO₂, nitrous oxide, methane, ozone and chlorofluorocarbons. These greenhouse gases are responsible for regulating the Earth's average temperature by absorbing and emitting radiation within the thermal infrared spectrum. One key difference between these various gases is their lifetime in the Earth's atmosphere. Reference 1 claims that the climate change resulting from increases in CO₂ is essentially irreversible for 1,000 years after the emissions cease.

Figure 1 shows the predicted CO₂ emission and associated global temperature increase.¹ Climate system responses are taken from Ref. 1 and assume a ramp of CO₂ emissions at a rate of 2%/year to peak CO₂ values of 450, 550, 650, 750, 850, and 1200 ppmv, followed by zero emissions. The rate of global fossil fuel CO₂ emission grew at ≈1%/year from 1980 to 2000 and >3%/year in the period from 2000 to 2005.¹ Warming over land is expected to be larger than the global averaged values. Also shown is the sea level rise (meters) from thermal expansion only (not including loss of glaciers, ice caps, or ice sheets).

Attempts to regulate the human production of greenhouse gases have been proposed but country participation is optional.⁴ With CO₂ emissions continuing to increase and no uniform global policy being enforced, deliberate human actions to mitigate the warming of the planet have been considered. One class of solutions that have been proposed is geo-engineering (GE). Geo-engineering is the application of technologically-based approaches that result in changes to planet properties. Although some oppose GE on the basis that these types of solutions take the

¹ Professor, Aerospace Engineering Department, AIAA fellow.

² Technical Assistant, Advanced Concepts Office, NASA MSFC, AIAA member.

pressure off changing the underlying problem of the world’s overdependence on fossil fuels for energy production, GE solutions should not be dismissed without consideration.

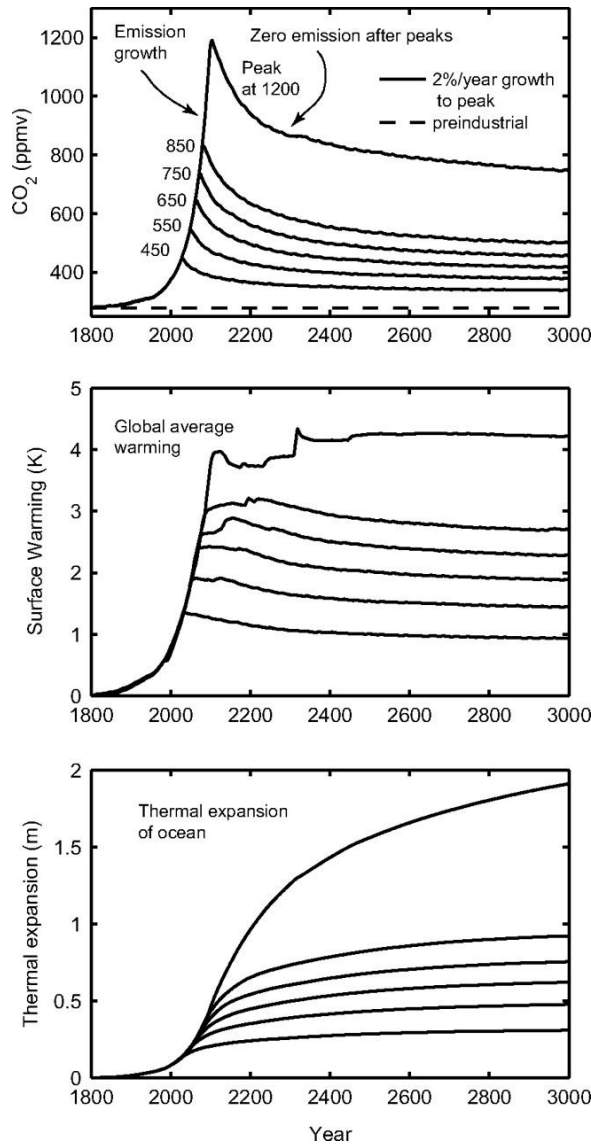


Figure 1. Carbon dioxide and global mean climate system changes (relative to preindustrial conditions in 1765.)¹

II. Solar Radiation Management of the Earth

Two main themes exist in GE research. The first is CO₂ removal and typically involves the seeding of clouds with chemicals that react with CO₂. The seeding can cause irreversible side-effects and damage (acid rain.) The second GE approach to climate change is to influence the energy balance equation of the Earth by reducing the amount of incoming solar radiation (SRM) and is the approach used here. SRM tactics use solar sunshades or parasols in space to redirect a portion of the incoming sunlight.

Reference 5 provides conceptual design on a sun shade near the Sun-Earth L₁ point that provides global shading. The solution presented requires a 700,000 km² reflective surface levitated in a non-Keplerian orbit with a radial distance inside the L₁ Sun-Earth location. The purpose of the shade is dual. Firstly, a reduction in the solar radiation by 3.4 W/m² is desired in an attempt to lower the Earth’s average temperature. Secondly, the reflective

shade would produce power to beam to Earth. This GE solution does address two very important issues but requires an enormous financial investment. The physical location and energy beaming requirements placed on the design increase launch costs and risk. A simpler GE solution is to design an earth-orbiting flotilla of shades with a single goal of solar radiation management.

Simulations indicate that geoengineering methods could markedly diminish regional and seasonal climate change from increased atmospheric CO₂, despite differences in radiative forcing patterns.⁶ Based on numerical modeling, the reduction of 4.17 W/m² of incident solar radiation would compensate the effect of a CO₂ doubling.⁶

Various earth orbiting SRM GE systems are presented with the objective to move the shade closer than the L₁ location thereby reducing costs and risks.

III. Global Shading Coverage

To predict the shade patterns cast upon the Earth, the physical dimensions of the sun must be modelled. An opaque body blocking light from a finite emitter produces three distinct regions- umbra, penumbra and antumbra. Figure 2 depicts these regions. The umbra is the darkest part of a shadow where the light source is completely blocked by the occluding body. The penumbra is the region in which only a portion of the light source is covered by the occluding body. The antumbra is the zone where the occluding body appears entirely contained within the sun's image.

The Earth's orbit about the sun defines the ecliptic plane. For global shading, it is optimal to locate the sunshade also in the ecliptic so that its shade with respect to the Earth is consistent. At a given moment, a horizontal axis along the Sun-Earth line can be defined. This axis is rotating about the sun with a period of one Earth year. The location of the shade with respect to this axis determines the shadow conditions on the Earth. In the GE solution proposed in Ref. 5, the height of the shade about the ecliptic is negligible (100s of Km) with respect to the sun's radius (7x10⁵ Km) and the distance the shade is from the sun (1.49x10⁸ Km) and the entire globe is shadowed in antumbra and the shade would appear as a dot on the sun, similar to an interior planet during transit.

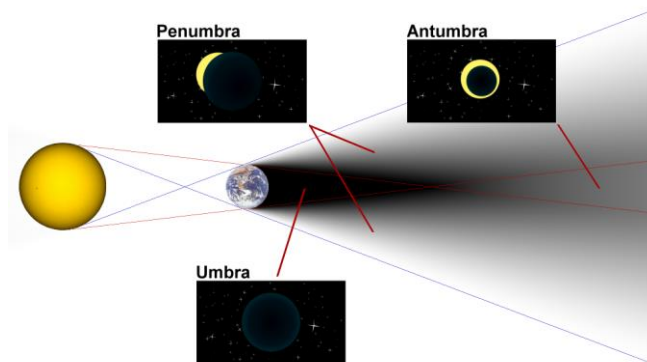


Figure 2: Umbra, Penumbra and Antumbra Definitions⁷.

If the shadow cone originates on the Sun-Earth line approximately 1.43 million kilometers from the Earth, it will grow to one earth radii when it intersects the Earth. As the shade is moved farther away from the Earth, the shadow cone encompasses space outside of the earth's radius and the shade is lost. As the shade moves closer to the Earth, the shade cone does not encompass the globe. In addition, this distance is within the Earth's gravity well and will not remain on the Sun-Earth line without constant radial acceleration. The magnitude of the required acceleration at 11 Earth radii is 0.08 m/s² in a radial direction away from the Earth. Several current technologies were investigated. Electrodynamic tethers can provide acceleration away from the Earth but are most efficient closer to the Earth's surface. The required acceleration mandated excessive amounts of current and tether lengths. Solar Electric Thruster could also provide the acceleration but the propellant usage limited any useful mission lifetimes.

IV. Localized Shading Coverage

A shade located within 1.43 million kilometers from the Earth will provide sub-global, regional shading. The shade's size and location depends on the desired percentage of blocked local energy, b and realized global blocked energy B . Consider the moon and a total solar eclipse as a natural inspiration. In a total solar eclipse, the disk of the

Sun is fully obscured by the Moon and $b=1$ but $B<1$. If the Moon were in a perfectly circular orbit, a little closer to the Earth, and orbited the Earth in the ecliptic plane, then there would be a total solar eclipse each orbit or once a month. However, the Moon's orbit is inclined at more than 5 degrees to the ecliptic, so the shadow cast when passing through the Sun-Earth plane usually misses the Earth.

To develop a relationship between the B and the shade area A_{sh} , the distance between the sun's subsolar point and the shade centroid must be defined using the variable x . To block b of sun's area, as the shade is brought closer to the earth the shade area decreases as x^2 . The antumbra shade on the earth is equal to A_{sh} surrounding the subsolar point resulting in Eq (1) where $B < b \leq 1$.

$$x = 224R_e * \sqrt{\frac{B}{b}} \quad (1)$$

For $B=0.25$ (3.4 W/m^2) and $b=1$ (total local blocking), $x=11.18 R_e$. Shade area is $320,000 \text{ km}^2$ which is less than the L1 solution but due to orbital mechanics, the shade will move away from the ideal position. Therefore, a constellation of satellites are required to maintain constant shading on the Earth.

V. Ring-World Regional Shade

An artist's rendering of a ring of shades that circles the Earth is shown in Figure 3. The ring-world concept will constantly maintain a shade on the Earth and Sun line. To size the shade area, the sun's image will be modeled as a circle as shown in Figure 4. Define the sun's area, A_s , and the rectangular area of the shade A_{sh} as seen by an observer on Earth assuming that the shield is always on the sun and earth line. To satisfy this assumption, orbital maintenance is required and is performed by the shade. If the shade is stationary with respect to the sun, a small reduction in the total irradiance of the sun by $b \text{ W/m}^2$ can be represented by Eq. (2).



Figure 3. A ring of sun shades.

$$\frac{A_{SH}}{A_s} = b \quad (2)$$

The average solar irradiance of the sun is 1367 W/m^2 . The sun's radius appears to fill a local radius of 0.276 degrees of the sky leading to the apparent area in degrees of $A_s=\pi(0.276^\circ)^2$

To cover the sun, the rectangular area of the shade is given as;

$$A_{SH}=4 * R_s * \Delta Z_{SH}^\circ = b * A_s = b\pi R_s^2 \quad (3)$$

Substituting values yields an angle in degrees.

$$\Delta Z_{SH}^\circ = 0.2 * b \quad (4)$$

In radians,

$$\Delta Z_{SH}^{\text{rad}} = b * 3.5 * 10^{-4} \quad (5)$$

The shade's height above the ecliptic plane in kilometers depends on the distance from the observer on Earth. In kilometers the shade height is then

$$\Delta Z_{SH}^{km} = x * \Delta Z_{SH}^{rad} \tag{6}$$

Next, define a non-dimensional variable K.

$$K = x / R_{earth} \tag{7}$$

For a sun shield to always be in between the sun and earth, a flotilla of discrete shades must form a ring in the ecliptic plane. This protective fleet of shades will be rotating faster or slower than the earth depending on the value of K. To form a ring around the earth, the required total number of shades is given by the integer round-off of $360 / 0.523 = 688$. Therefore the total area of the ring,

$$A_r = 688 * A_{sh} \tag{8}$$

R_s^{km} is the sun's apparent radius to the observer in kilometers.

$$A_{sh} = 2.6 * 10^3 * b * K^2 \tag{9}$$

Substituting equation (9) into equation (8) yields an expression for the total area of the ring.

$$A_r = 1.8 * 10^6 * b * K^2 \text{ km}^2 \tag{10}$$

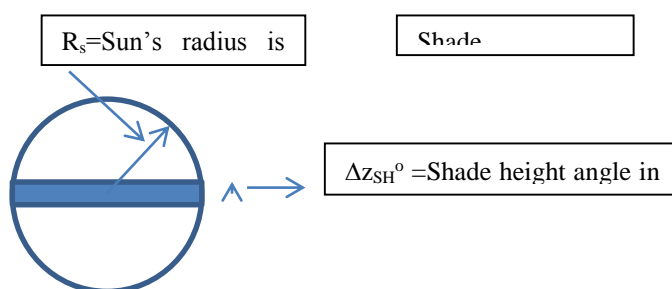


Figure 4: Simplified Geometry of Sun and Shade.

VI. Elliptical Orbit Regional Shades

Elliptic orbits were investigated as candidates for the regional shades. A unique orbit that provides consistent daily shading of the Earth's surface was discovered. The orbital characteristics include a 24-hour period with 16 hours in sunlight. The orbit is retrograde with perigee at local mid-night provides at substantial hang-time around the Sun-Earth line. Sixteen shades provide 24-hours shading of the sub-solar point. Figure 5 captures constellation. In this figure the sun is located along the apogee line.

The slowly rotating sail is used to distribute the shade about the ecliptic plane. The reflecting sails provide thrust to maintain the proper orbital alignment. Each individual shade is sized via Eq. (9). For equivalent regional shading b, the required sail area is an order of magnitude less than that of the orbital ring presented above.

VII. In-Space Mean Solar Irradiance Measurements

A typical value for the solar constant is 1367 W/m^2 but the solar energy output is not constant. In-space radiation measurements fluctuate on the order 0.1%.⁸ Sun shades must be capable of blocking more radiation than 0.1% in order to have any meaningful control of the energy input into the Earth's system. Figure 6 displays data of solar radiation measured by spacecraft between the years 1979-1999.⁸ The data is measured in a plane normal to the incident rays. The solid line shows the filtered trend. The sun's energy production is dynamic and is not completely understood. The output follows the well-known 11-year cycle and energy output has been correlated with the presence or absence of sun spots.

VIII. Elliptical Orbit GE Shade Design

Geosynchronous orbits have a period of 24 hours and in two-body dynamics return to the original state after completing one revolution about the Earth. A value of $K=6.61$ defines the orbit size. The perigee radius is between $1.2 \leq K \leq 2$ to avoid orbital debris. Apogee occurs between $11 \leq K \leq 12$. Orbital inclination aligns with the ecliptic plane and oscillates between $\pm 23.4^\circ$ depending on the time of year. A reduction of 0.25% or 3.4 W/m^2 is desired. Each shade has an area $A_{sh}=940 \text{ Km}^2$. The total ring area at $K=6.61$ is $A_r=644,000 \text{ Km}^2$ while the 16 satellite constellation is $15,000 \text{ km}^2$, an order of magnitude reduction for regional shading. Global reduction of 3.4

W/m^2 is achieved by using 50 different orbital inclinations each with 16 satellites. Total blocking area is increased by 50 fold to $750,000 \text{ km}^2$. The individual shade areas most likely will be groups of smaller sails working as a group to redirect the sun's energy.



Figure 5. Constellation of 16 Shades in Elliptic Orbit.

IX. Advanced Metamaterials

The cost of launching a system of shades is linearly proportional to the total system launch mass. The shades large reflective surface dominates the shade design so any reduction in reflective material areal density is magnified. Recent advances in nanosheet technology have produced areal densities of $2.6 \times 10^{-2} \text{ g/m}^2$ of transparent material.⁹ Silver nanoparticles have been combined with various composites into nanosheets that produce reflective characteristics.^{10,11} In Ref. 11, the thickness of a 2D silver nanosheet is stated to be $1.9 \times 10^{-9} \text{ m}$. Assuming that the thickness is entirely Silver (an approximation), the areal density of this particular 2D silver nanosheet is estimated to be the material density of silver multiplied by the sheet thickness or 0.02 g/m^2 . Reference 11 also graphs absorptive and reflective properties versus optical wavelengths for 1-5 layers of 2D nanosheets. For wavelengths greater than 750 nm, 5 layers provides approximately 100% reflectivity. However, as the wavelength decreases so does reflectivity. From the graph it appears that the reflectivity is about 40% for 500nm and drops to near zero at 300nm. By combining multiple layers of silver nanosheets with different percentages of silver versus composite materials, a resulting reflective surface tailored to redirect a given range of wavelengths can be engineered. In the near future, a full spectrum reflector can be produced by fusing 10 layers of metamaterials. If each layer is approximated by the density of the 2D silver nanosheet, then the resulting areal density is 0.2 g/m^2 thereby greatly reducing the total launch mass of the shade system.

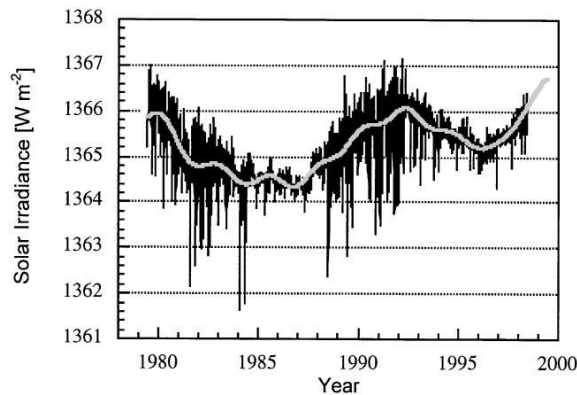


Figure 6. Measurement of Solar Irradiance.

X. Demonstrator Mission

One noteworthy aspect to the earth orbiting regional sunshade is that it is scalable. As shown in Eq. (9), the sail area scales linearly with b , the local blocked energy percentage. A demonstrator mission with $b=0.001$ could be flown as an experiment in LEO. Using equation (9), a single shade area is approximately 4 km^2 . Using a near term value for the reflective material areal density of 1 g/m^2 yields a shade mass of 4,000 kg. Adding the deployment system and spacecraft mass yield a launch mass of approximately 5,000kg. Assume an optimistic negotiation with the launch company results in a contract of \$5000/kg. A demonstrator mission could be launched for \$25 M. Total estimated design, development, test, and evaluation for delivery to launch pad is estimated as \$25M leading to a total cost for a demonstrator mission of approximately \$50M, well within the constraints of many government and commercial industry financial budgets.

Figure 7 depicts the concentration of human population by latitude. The population distribution centers around 30 N latitude. The first demonstration mission may want to target this region.

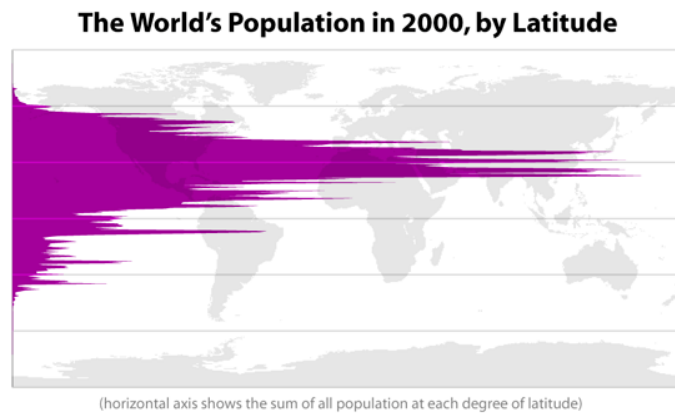


Figure 7. Concentration of Human Population

XI. Conclusion

Earth orbiting sunshades designed to reduce the amount of solar energy that is transmitted to the Earth's surface is presented. The approach outlined is scalable in terms of redirected energy and distance from the earth. Although global shading requires tremendous financial investment, a regional shading solution that would provide weather modification is feasible. A demonstrator mission that would serve as an experiment of the concept is well within many organization's financial budgets.

Acknowledgments

The authors thank the NASA Marshall Space Flight Center's Summer Faculty Fellow programs that allowed them the opportunity to collaborate.

References

- ¹ Solomon, S. et al., "Irreversible Climate Change Due to Carbon Dioxide Emissions," *Proceedings of the National Academy of Sciences*, Vol. 106, No. 6, 2009, pp. 1704-1709, doi: 10.1073/pnas.0812721106; available online July 8, 2015 at http://www.pnas.org/content/106/6/1704.full?wptouch_preview_theme=enabled
- ² Canadell, J., et al., "Contributions to Accelerating Atmospheric CO₂ Growth from Economic Activity, Carbon Intensity, and Efficiency of Natural Sinks," *Proceedings of the National Academy of Sciences*, Vol 104, No. 47, pp. 18866-18870, doi:10.1073/pnas.0702737104; available online July 8, 2015 at <http://www.pnas.org/content/104/47/18866.full.pdf+html-pmid=17962418-pmc=2141868>
- ³ Raupach, M., et al., "Global and Regional Drivers of Accelerating CO₂ Emissions," *Proceeding of the National Academy of Sciences*, Vol. 104, No. 24, pp. 10288-10293; doi:10.1073/pnas0700609104. Available online July 8, 2015 at <http://www.pnas.org/content/104/24/10288.full?hits=10>

⁴ Oberthur, S. and H. Ott, “The Kyoto Protocol: International Climate Policy for the 21st Century,” Springer Science and Business Media, 1999.

⁵ Kennedy, R. G. III, et al., “Dyson Dots and Geoengineering: The Killer App”, *Journal of the British Interplanetary Society*, Vol. 66, No. 10/11, 2013.

⁶ Govindasamy, B. and K. Caldeira, “Geoengineering Earth's Radiation Balance To Mitigate CO₂-Induced Climate Change,” *Geophysical Research Letters*, Vol. 27, No. 14, 2000, pp. 2141-2144.

⁷ "Diagram of umbra, penumbra & antumbra" by Qarnos - Own work. Licensed under Public Domain via Wikimedia Commons - https://commons.wikimedia.org/wiki/File:Diagram_of_umbra,_penumbra_%26_antumbra.png#/media/File:Diagram_of_umbra,_penumbra_%26_antumbra.png

⁸ Beer, J. W. Mende and R. Stellmacher, “The Role of the Sun in Climate Forcing,” *Quaternary Science Reviews*, Vol. 19, pp. 403-415, 2000.

⁹ Zhang, M., et al., “Strong Transparent Multifunctional Carbon Nanotube Sheets,” *Science*, Vol 309, No. 5738, 2005, pp. 1215-1219: doi:10.1126/science.1115311. Available online July 8 2015 at <http://www-eng.lbl.gov/~shuman/NEXT/MATERIALS%26COMPONENTS/CNTsheets.pdf>

¹⁰ Kharlampieva, E., et al., “Flexible Silk-Inorganic Nanocomposites: From Transparent to Highly Reflective,” *Advanced Functional Materials*, No. 20, 2010, pp. 840-846. Available online on July 8, 2015 at <http://www.dtic.mil/dtic/tr/fulltext/u2/a577957.pdf>

¹¹ Okamoto, K., et al., “Tuning Colors of Silver Nanoparticle Sheets By Multilayered Crystalline Structure on Metal Substrates,” *Plasmonics*, No. 8, 2013, pp. 581-590. Doi:10/1007/s11468-9437-2. Available online July 8, 2015 at http://www.plasmonic.net/Documents/Plasmonics_8_581-2013.pdf